

# Theoretical Messenger Spectroscopy of Microsolvated Hydronium and Zundel Cations\*\*

Marcel Baer, Dominik Marx, and Gerald Mathias\*

Among the most ubiquitous ions in aqueous solutions are solvated protons,  $\text{H}^+(\text{aq})$ , which are of fundamental importance from solution chemistry to enzymatic processes. The two archetypal protonated water complexes, the  $\text{H}_3\text{O}^+$  (hydronium ion) and  $\text{H}_5\text{O}_2^+$  (Zundel cation), are not only the basic building blocks of more complex transient networks in condensed phases,<sup>[1]</sup> but have a right of their own in fields such as cluster science and atmospheric chemistry, to name but two. Therefore, finite  $\text{H}^+(\text{H}_2\text{O})_n$  complexes have been the focus of a plethora of investigations.<sup>[2–10]</sup> Improvements in vibrational spectroscopy, and in particular sophisticated action spectroscopic methods based on messenger predissociation and multiphoton dissociation, allow unprecedented insights into such species.<sup>[11,12]</sup> However, the interpretation of messenger spectra is by no means straightforward owing to interactions of the parent molecules with tagging species, such as  $\text{H}_2$ , Ar, or Ne.

In pioneering experiments, Y. T. Lee and co-workers studied the hydronium and Zundel cations in the spectral range above  $3100\text{ cm}^{-1}$  by  $\text{H}_2$  microsolvation.<sup>[3,13,14]</sup> These spectra showed that interactions between the messenger species and these cations significantly modify the spectra. Recent high-resolution vibrational predissociation measurements using Ar or Ne adducts now access the full IR fingerprint region down to  $600\text{ cm}^{-1}$ .<sup>[7,15–18]</sup> However, important spectral features, such as the characteristic double band of the proton-transfer mode or the number of bands in the O–H stretching region, differ significantly and depend heavily on the experimental method that is employed.<sup>[3–5,13,16]</sup>

In a tour de force full-dimensional quantum dynamics calculation (MCTDH), the comprehensive spectral assignment of the bare Zundel cation has been recently accomplished by H.-D. Meyer and co-workers, which explains the aforementioned challenging double band near  $1000\text{ cm}^{-1}$  as being a Fermi resonance.<sup>[9]</sup> However, such very precise

calculations appear to be currently unfeasible for micro-solvated  $\text{H}_5\text{O}_2^+$  adducts, thus leaving open a wealth of questions on the assignment of such action spectra.

Herein we extensively use ab initio molecular dynamics (AIMD)<sup>[19]</sup> to compute and assign the IR spectra for  $\text{H}_2$ -microsolvated hydronium and Zundel cation adducts. The AIMD approach to theoretical vibrational spectroscopy<sup>[20–23]</sup> has been demonstrated specifically for bare  $\text{H}_5\text{O}_2^+$  itself<sup>[24–27]</sup> to compare favorably with traditional approaches based on qualitative assessments. Herein, using AIMD trajectories, approximate normal modes are determined which supply a full set of optimized vibrational coordinates that represent the fundamental modes;<sup>[23,28]</sup> details are given in the Supporting Information.

As will be demonstrated, the interpretation of the complex messenger spectra requires explicit inclusion of the tagging species. Anticipating our key results, we show how messenger species qualitatively change IR spectra of adducts and how this renders their intuitive assignment based on the parent spectra ambiguous. Specifically, for the fluxional Zundel cation,  $[\text{H}_2\text{O}\cdots\text{H}\cdots\text{OH}_2]^+$ , an interpretation of messenger spectra in terms of a weighted mixture of tightly bound  $\text{H}_5\text{O}_2^+\cdots\text{H}_2$  and weakly bound  $\text{H}_5\text{O}_2^+\cdots\text{H}_2$  adducts, instead of symmetry-breaking  $[\text{H}_2\text{O}\cdots\text{H}\cdots\text{OH}_2]^+\cdots\text{H}_2$  due to tagging,<sup>[3]</sup> is shown to consistently explain the different action spectra. This concept will be of broad relevance beyond this specific case.

First insights into messenger-induced changes to spectra are provided by the well-understood hydronium cation<sup>[2,29,30]</sup> (Figure 1). The calculated IR spectrum of bare  $\text{H}_3\text{O}^+$  (black in Figure 1a) spans a broad frequency window of about  $250\text{ cm}^{-1}$  in the O–H stretching region. It convincingly matches the range and shape of the experimental rovibrational absorptions of the asymmetric stretching modes (blue).<sup>[2]</sup> The power spectra of the two asymmetric stretching modes  $\nu_a$  and  $\nu_a'$  (blue, green) yield narrow bands, both at  $3506\text{ cm}^{-1}$ , which is very close to the measured effective stretching frequencies of  $3519\text{ cm}^{-1}$  and  $3536\text{ cm}^{-1}$ .<sup>[2]</sup> The IR-inactive symmetric stretching mode  $\nu_s$  is found at  $3418\text{ cm}^{-1}$  (red). Thus, the coupling to overall rotation significantly broadens the absorption of the asymmetric stretches to the range observed in experiment.

A strikingly modified IR spectrum is observed for the  $\text{H}_3\text{O}^+(\text{H}_2)_2$  adduct. The computed spectrum in Figure 1b again convincingly reproduces the experimental spectrum in all respects. In particular, only one band remains in the stretching region of the parent,  $\text{H}_3\text{O}^+$ , which can be reliably assigned to the free O–H stretching vibration<sup>[13]</sup>  $\nu_f$ : its power spectrum (red) coincides with the IR peak. However, upon attaching two  $\text{H}_2$  species, two new, red-shifted bands emerge

[\*] M. Baer, D. Marx, G. Mathias  
Lehrstuhl für Theoretische Chemie, Ruhr-Universität Bochum  
44780 Bochum (Germany)

G. Mathias  
Lehrstuhl für BioMolekulare Optik  
Ludwig-Maximilians-Universität München  
Oettingenstrasse 67, 80538 München (Germany)  
E-mail: gerald.mathias@physik.uni-muenchen.de

[\*\*] We are grateful to Research Department Interfacial Systems Chemistry (RD IFSC), Deutsche Forschungsgemeinschaft (DFG), and Fonds der Chemischen Industrie (FCI) for partial financial support as well as to BOVILAB@RUB (Bochum) and Ressourcenverbund NRW for computational resources.

Supporting information for this article is available on the WWW under <http://dx.doi.org/10.1002/anie.201001672>.

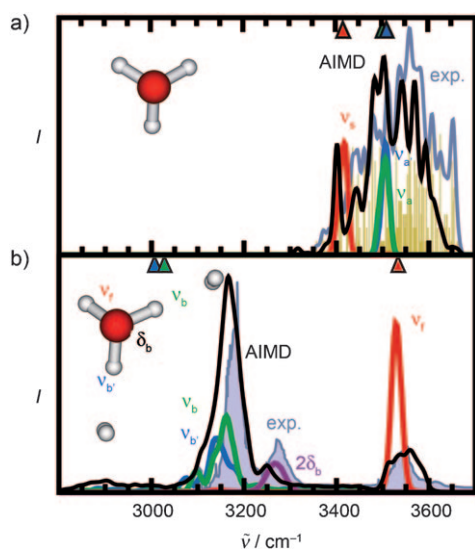


**Figure 1.** Comparison of a) the O-H stretching vibration region of the bare hydronium ion to b) the microsolvated  $\text{H}_3\text{O}^+(\text{H}_2)_2$ . Black lines are the theoretical IR spectra at 150 K. The blue line in (a) is a broadened absorption spectrum obtained by convoluting the resolved rovibrational resonances<sup>[2]</sup> (yellow) by small Gaussian functions; the blue spectrum in (b) is the experimental predissociation action spectrum<sup>[13]</sup> of  $\text{H}_3\text{O}^+(\text{H}_2)_2$ . The remaining lines are power spectra of linear combinations of internal coordinates (see text and insets), and triangles mark the harmonic frequencies using the same color code.

at 3151 and 3234  $\text{cm}^{-1}$ , which are again close to the experimental peaks at 3180 and 3275  $\text{cm}^{-1}$ . Intuitively, it is tempting to assign them to the remaining two  $\text{H}_2$ -bonded individual O-H stretching modes  $\nu_b$  and  $\nu_b'$ ,<sup>[13]</sup> but their power spectra (peaks at 3162 and 3141  $\text{cm}^{-1}$ ; green and blue) contribute exclusively to the prominent band at 3151  $\text{cm}^{-1}$ , whereas they yield no bands at 3234  $\text{cm}^{-1}$ .

The correct assignment is only obtained after considering the frequency-doubled bend  $\delta_b$  (fundamental at 1633  $\text{cm}^{-1}$ ) involving the  $\text{H}_2$ -bonded protons in the core. Its position and width (purple line) closely matches the prominent sideband around 3234  $\text{cm}^{-1}$ , which we thus assign to a bend overtone. All this demonstrates that even in a small and quasi-rigid molecule, the addition of messenger molecules induces intricate modifications of the IR spectrum of the parent molecule.

What are then the messenger-species-induced changes for the tagged Zundel ion  $\text{H}_5\text{O}_2^+\text{H}_2$ , in which the parent Zundel ion is a fluxional molecule? The AIMD reference spectrum for bare  $\text{H}_5\text{O}_2^+$  and the assigned modes in the O-H stretching region are shown in Figure 2 $\beta$ . The two AIMD IR bands feature the same shape as the IR multiphoton dissociation (IRMPD) data<sup>[3]</sup> of bare  $\text{H}_5\text{O}_2^+$ , but they are slightly red-shifted, whereas the MCTDH spectrum<sup>[9,31]</sup> is slightly blue-shifted (Figure 2 $\alpha$ ). The AIMD-based mode analysis<sup>[23,28]</sup> readily yields the gerade  $\nu_{\text{sg}}$  and ungerade  $\nu_{\text{su}}$  combination of the symmetric stretching mode of both water moieties and the degenerate combinations of the asymmetric stretching modes  $\nu_a$  and  $\nu_a'$ , alike the MCTDH assignment.<sup>[31]</sup>

$\text{H}_2$  tagging induces an overall red-shift of the  $\text{H}_5\text{O}_2^+\text{H}_2$  stretches (Figure 2 $\delta$ ). The symmetry-breaking that is induced upon adduct formation localizes the symmetric and asym-

metric stretches on the  $\text{H}_2$ -bonded ( $\nu_{\text{sb}}$ ,  $\nu_{\text{ab}}$ ) and free ( $\nu_{\text{sf}}$ ,  $\nu_{\text{af}}$ ) water moieties. This mode assignment (red, violet, green, blue lines) reproduces all of the band positions and shapes of the calculated IR absorptions in Figure 2 $\delta$  well. However, the experimental messenger spectrum of  $\text{H}_5\text{O}_2^+\text{H}_2$  (Figure 2 $\epsilon$ ; blue line, shaded region) features a much richer lineshape and looks qualitatively different: only the  $\sigma_1$  and  $\sigma_3$  peaks match the calculated symmetric and asymmetric vibrations, respectively, including their band shapes due to sub-bands corresponding to bonded and free water;  $\nu_{\text{sb}}$  and  $\nu_{\text{sf}}$  merge into one skewed peak (corresponding to  $\sigma_1$ ) at elevated temperatures. In contrast, the remaining peaks  $\sigma_2$  and  $\sigma_4$  come close to the stretching vibrations of the bare Zundel ion,<sup>[3]</sup> both in AIMD and IRMPD<sup>[3]</sup> (Figure 2 $\beta$  and 2 $\alpha$ , respectively). Thus, tentatively, the experimental messenger spectrum of the  $\text{H}_2$ -tagged species might be explained by assuming a mixture of tightly bound  $\text{H}_5\text{O}_2^+\text{H}_2$  and weakly bound  $\text{H}_5\text{O}_2^+\cdots\text{H}_2$  adducts, where the latter would essentially contribute the same signal as bare  $\text{H}_5\text{O}_2^+$  ion.

This hypothesis differs distinctly from the tentative earlier interpretation, which assigned the four peaks  $\sigma_1$  to  $\sigma_4$  to the four stretching modes of a single tightly bound adduct. This predicts a splitting of 89  $\text{cm}^{-1}$  for the symmetric stretching assigned to  $\sigma_1$  and  $\sigma_2$  due to  $\text{H}_2$  tagging, whereas AIMD yields only 40  $\text{cm}^{-1}$ , and earlier harmonic estimates give a value of 53  $\text{cm}^{-1}$ <sup>[32]</sup>. Experimentally it has been observed that in the  $\text{H}_2$  adduct, the shared proton is systematically shifted away from the  $\text{H}_2$  bond side, that is, the free water acquires some hydronium ion character:  $[\text{H}_2\text{O}\cdots\text{H}\cdots\text{OH}_2]^+\text{H}_2$ . However, from AIMD, the free energy minimum of the shared proton displayed in Figure 2e) is only negligibly shifted (by ca. 0.01 Å) in that direction. Moreover, such a nearly symmetric proton-transfer profile does not support a substantial shift due to zero-point motion either.

Figure 2 $\epsilon$  also shows that the stretching region of the Ar-tagged complex matches the  $\text{H}_5\text{O}_2^+\text{H}_2$  messenger spectrum strikingly closely,<sup>[16]</sup> whereas the Ne-tagged complex recovers the IRMPD spectrum<sup>[3]</sup> of bare  $\text{H}_5\text{O}_2^+$ .<sup>[16]</sup> It should be noted that AIMD simulations of the Ar-tagged complex also yield only two IR absorption peaks in the O-H stretch region.<sup>[26]</sup> Thus, also for the Ar-tagged Zundel complex, our findings predict a similar mixture of tightly and weakly bound adducts, whereas the Ne-tag apparently does not noticeably perturb the bare Zundel ion spectrum.<sup>[16]</sup>

Similar effects are observed for the doublet structure at about 1000  $\text{cm}^{-1}$  (Figure 2e), which has been assigned by MCTDH for the bare Zundel ion to a Fermi resonance of the proton-transfer fundamental and a combination of lower frequency modes<sup>[9]</sup> (see Figure 2e and 2a). This observation matches the measured Ne messenger spectrum well. In stark contrast, the spectrum of the Ar-tagged species features one additional sideband for each doublet peak.<sup>[16]</sup> Akin to the O-H stretching region, the position and shape of two of these peaks closely agree with those of the spectrum for the Ne-tagged species,<sup>[16]</sup> which again hints to a mixture of tightly and weakly bound species for the Ar-Zundel ion adduct.

More insights into the effects of tagging are gained by analyzing the prominent doublet band of AIMD spectra of the untagged versus tagged species. The AIMD reference

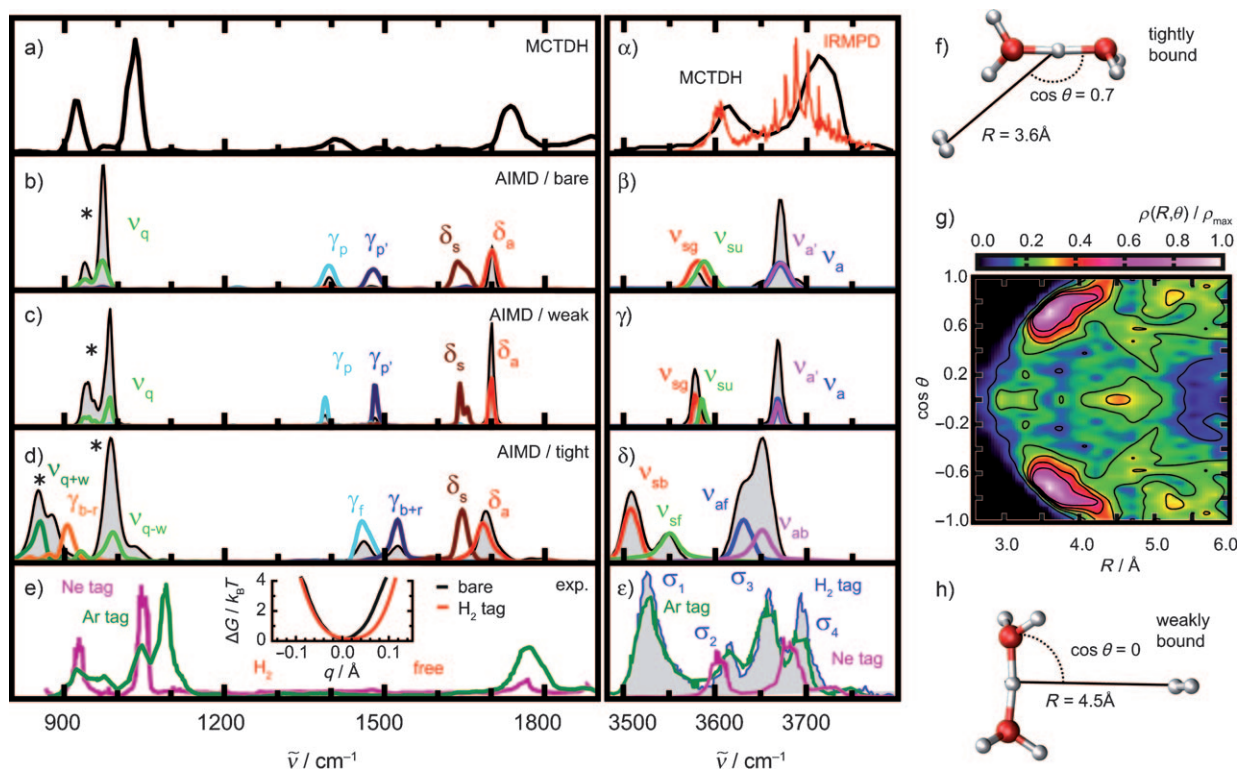


**Figure 2.** Comparison of experimental and calculated vibrational spectra for bare and various messenger-tagged  $\text{H}_3\text{O}_2^+$  cations. The theoretical AIMD IR spectra at 10 K for bare  $\text{H}_3\text{O}_2^+$  and the weakly bound ( $\text{H}_3\text{O}_2^+\cdots\text{H}_2$ ) and tightly bound ( $\text{H}_3\text{O}_2^+\cdots\text{H}_2$ ) adducts are shown by gray shaded areas in (b/β), (c/γ), and (d/δ), respectively. Colored lines show power spectra of approximate normal coordinates:  $\nu_{\text{si,al}}$  symmetric and asymmetric O-H stretches,  $\delta_{\text{g,u}}$  gerade/ungerade combinations of the water bending modes,  $\gamma_i$  proton out-of-axis vibration, and  $\nu_q$  proton-transfer motion (marked with \*); see text and Supporting Information for details. a/α) The MCTDH<sup>[9]</sup> benchmark IR spectrum of bare  $\text{H}_3\text{O}_2^+$  (black) and the bare  $\text{H}_3\text{O}_2^+$  IRMPD<sup>[3]</sup> OH-stretching region (red). e/ε) Experimental messenger spectra for  $\text{H}_3\text{O}_2^+\cdots\text{Ar}$  (green),<sup>[16]</sup>  $\text{H}_3\text{O}_2^+\cdots\text{Ne}$  (purple),<sup>[16]</sup> and  $\text{H}_3\text{O}_2^+\cdots\text{H}_2$  (shaded area with blue outline).<sup>[13]</sup> The inset (e) is the computed free-energy profile  $\Delta G$  along the proton-transfer coordinate  $q = r_{\text{OH}^+} - r_{\text{O}^+\text{H}}$  for the bare (black) and  $\text{H}_2$ -tagged (red) Zundel cations from (b/β) and (d/δ); for the latter, the axis labels  $\text{H}_2$  and free (in red) indicate towards which water moiety the proton is shifted. g) Normalized and symmetrized probability distribution  $\rho(R, \theta)/\rho_{\text{max}}$  of  $\text{H}_2$ -Zundel adduct structures (in the plane spanned by  $R$  and  $\cos\theta$  as defined in (f)) obtained from a superposition of restrained AIMD runs (see the Supporting Information for details). f, h) Typical structures of tightly bound and weakly bound adducts according to the most pronounced maxima of  $\rho(R, \theta)$ .

spectrum of the bare  $\text{H}_3\text{O}_2^+$  ion (Figure 2b) also has this doublet at about  $1000\text{ cm}^{-1}$ , which is assigned to proton-transfer motion  $\nu_q$  and merges to a single peak at higher temperatures.<sup>[25–27]</sup> We note that the other fundamental vibrations found by AIMD in the fingerprint region as assigned by MCTDH show similar character.<sup>[9,31,33,34]</sup> However, tagging effects are found to be dramatic for the  $1000\text{ cm}^{-1}$  proton-transfer mode (Figure 2d). The splitting is significantly increased, and our mode analysis now reveals two fundamentals: the in-phase and out-of-phase coupling of the proton-transfer coordinate to the wagging mode of the free water moiety,  $\nu_{q+w}$  and  $\nu_{q-w}$ , which are similar to the coupling pattern revealed by MCTDH for the wagging overtones of bare Zundel ions:<sup>[9]</sup> for  $\text{H}_3\text{O}_2^+$ , a Fermi resonance is found<sup>[9]</sup> that is beyond our AIMD-based approach. In conclusion, the symmetry-breaking induced by  $\text{H}_2$  tagging directly couples the low-frequency wagging motion to proton transfer.

Finally, what could the weakly bound adducts look like? In the tightly bound adduct, which clearly dominates the low-

temperature simulations (Figure 2d,δ), the  $\text{H}_2$  moiety strongly interacts with one proton of a water molecule (Figure 2f). Starting from this structure, we conducted a series of AIMD simulations at 150 K for which we restrained the minimal distance of  $\text{H}_2$  to any Zundel proton to a given value, which is increased systematically to enforce exploration of less favorable conformations (see the Supporting Information for details). The resulting probability  $\rho(R, \theta)$  of finding  $\text{H}_2$  at a distance  $R$  from the center of the two Zundel oxygen atoms and an angle  $\theta$  with respect to the O-O axis is provided in Figure 2g. The tightly bound adduct is found at  $R \approx 3.6\text{ Å}$  and  $\cos\theta \approx \pm 0.7$ , which corresponds to the global maximum. Orthogonal to the O-O axis, that is, for  $\cos\theta \approx 0$ , we find indeed a significant local maximum near  $R \approx 4.5\text{ Å}$ ; a representative structure is given in Figure 2h). The corresponding low-temperature IR spectrum and the mode assignments are shown in Figure 2c,γ. Indeed, the resulting spectrum is essentially identical to the one of bare Zundel ion in Figure 2b,β. Thus, the structure in Figure 2h is a promising candidate for the postulated weakly bound adduct,

being an intermediate explored by the H<sub>2</sub> moiety upon dynamically exchanging one water molecule of the H<sub>3</sub>O<sub>2</sub><sup>+</sup> core by the other, and thus converting one tightly bound adduct into a degenerate form.

Received: March 19, 2010

Revised: June 6, 2010

Published online: August 23, 2010

**Keywords:** cations · density functional calculations · microsolvation · vibrational spectroscopy · Zundel cations

- [1] D. Marx, *ChemPhysChem* **2006**, *7*, 1848–1870, Addendum: *ChemPhysChem* **2007**, *8*, 209–210.
- [2] M. H. Begemann, R. J. Saykally, *J. Chem. Phys.* **1985**, *82*, 3570–3579.
- [3] L. I. Yeh, M. Okumura, J. D. Myers, J. M. Price, Y. T. Lee, *J. Chem. Phys.* **1989**, *91*, 7319–7330.
- [4] K. R. Asmis, N. L. Pivonka, G. Santambrogio, M. Brummer, C. Kaposta, D. M. Neumark, L. Woste, *Science* **2003**, *299*, 1375–1377.
- [5] T. D. Fridgen, T. B. McMahon, L. MacAleese, J. Lemaire, P. Maitre, *J. Phys. Chem. A* **2004**, *108*, 9008–9010.
- [6] M. Miyazaki, A. Fujii, T. Ebata, N. Mikami, *Science* **2004**, *304*, 1134–1137.
- [7] J. M. Headrick et al., *Science* **2005**, *308*, 1765–1769.
- [8] G. Niedner-Schatteburg, *Angew. Chem.* **2008**, *120*, 1024–1027; *Angew. Chem. Int. Ed.* **2008**, *47*, 1008–1011.
- [9] O. Vendrell, F. Gatti, H.-D. Meyer, *Angew. Chem.* **2007**, *119*, 7043–7046; *Angew. Chem. Int. Ed.* **2007**, *46*, 6918–6921.
- [10] O. Vendrell, F. Gatti, H.-D. Meyer, *Angew. Chem.* **2009**, *121*, 358–361; *Angew. Chem. Int. Ed.* **2009**, *48*, 352–355.
- [11] E. J. Bieske, O. Dopfer, *Chem. Rev.* **2000**, *100*, 3963–3998.
- [12] N. C. Polfer, J. Oomens, *Mass Spectrom. Rev.* **2009**, *28*, 468–494.
- [13] M. Okumura, L. I. Yeh, J. D. Myers, Y. T. Lee, *J. Phys. Chem.* **1990**, *94*, 3416–3427.
- [14] L. I. Yeh, Y. T. Lee, J. T. Hougen, *J. Mol. Spectrosc.* **1994**, *164*, 473–488.
- [15] J. M. Headrick, J. C. Bopp, M. A. Johnson, *J. Chem. Phys.* **2004**, *121*, 11523–11526.
- [16] N. I. Hammer et al., *J. Chem. Phys.* **2005**, *122*, 244301.
- [17] E. G. Diken, J. M. Headrick, J. R. Roscioli, J. C. Bopp, M. A. Johnson, A. B. McCoy, *J. Phys. Chem. A* **2005**, *109*, 1487–1490.
- [18] L. R. McCunn, J. R. Roscioli, M. A. Johnson, A. B. McCoy, *J. Phys. Chem. B* **2008**, *112*, 321–327.
- [19] D. Marx, J. Hutter, *Ab Initio Molecular Dynamics: Basic Theory and Advanced Methods*, Cambridge University Press, Cambridge, **2009**.
- [20] R. Rousseau, V. Kleinschmidt, U. W. Schmitt, D. Marx, *Angew. Chem.* **2004**, *116*, 4908–4911; *Angew. Chem. Int. Ed.* **2004**, *43*, 4804–4807.
- [21] O. Asvany, P. P. Kumar, B. Redlich, I. Hegemann, S. Schlemmer, D. Marx, *Science* **2005**, *309*, 1219–1222.
- [22] G. Mathias, D. Marx, *Proc. Natl. Acad. Sci. USA* **2007**, *104*, 6980–6985.
- [23] S. D. Ivanov, O. Asvany, A. Witt, E. Hugo, G. Mathias, B. Redlich, D. Marx, S. Schlemmer, *Nat. Chem.* **2010**, *2*, 298–302.
- [24] M. V. Vener, O. Kühn, J. Sauer, *J. Chem. Phys.* **2001**, *114*, 240–249.
- [25] J. Sauer, J. Dobler, *ChemPhysChem* **2005**, *6*, 1706–1710.
- [26] M. Park, I. Shin, N. J. Singh, K. S. Kim, *J. Phys. Chem. A* **2007**, *111*, 10692–10702.
- [27] M. Kaledin, A. L. Kaledin, J. M. Bowman, J. Ding, K. D. Jordan, *J. Phys. Chem. A* **2009**, *113*, 7671–7677.
- [28] G. Mathias, M. Baer, unpublished results.
- [29] X. C. Huang, S. Carter, J. Bowman, *J. Chem. Phys.* **2003**, *118*, 5431–5441.
- [30] F. Dong, D. Nesbitt, *J. Chem. Phys.* **2006**, *125*, 144311.
- [31] O. Vendrell, F. Gatti, H.-D. Meyer, *J. Chem. Phys.* **2007**, *127*, 184303.
- [32] E. Bosch, M. Moreno, J. M. Lluch, *J. Chem. Phys.* **1992**, *97*, 6469–6471.
- [33] O. Vendrell, M. Brill, F. Gatti, D. Lauvergnat, H. D. Meyer, *J. Chem. Phys.* **2009**, *130*, 234305.
- [34] O. Vendrell, F. Gatti, H. D. Meyer, *J. Chem. Phys.* **2009**, *131*, 034308.